quantum beam science

MDPI

Article

Effects of Energetic Carbon-Cluster Ion Irradiation on Lattice Structures of $EuBa_2Cu_3O_{7-x}$ Oxide Superconductor

Akihiro Iwase [1,2,*], Yuichi Saitoh [3], Atsuya Chiba [3], Fuminobu Hori [2] and Norito Ishikawa [4]

[1] The Wakasa Wan Energy Research Center (WERC), Tsuruga 914-0192, Fukui, Japan
[2] Graduate School of Engineering Division of Quantum and Radiation Engineering, Osaka Metropolitan University (OMU), Sakai 599-8531, Osaka, Japan; horif@omu.ac.jp
[3] National Institutes for Quantum Science and Technology (QST), Takasaki 370-1292, Gunma, Japan; saito.yuichi@qst.go.jp (Y.S.); chiba.atsuya@qst.go.jp (A.C.)
[4] Japan Atomic Energy Agency (JAEA), Tokai 319-1195, Ibaraki, Japan; ishikawa.norito@jaea.go.jp
* Correspondence: aiwase@werc.or.jp

Abstract: C-axis-oriented $EuBa_2Cu_3O_{7-x}$ oxide films that were 100 nm thick were irradiated with 0.5 MeV C monoatomic ions, 2 MeV C_4 cluster ions and 4 MeV C_8 cluster ions at room temperature. Before and after the irradiation, X-ray diffraction (XRD) measurement was performed using Cu-Ka X-ray. The c-axis lattice constant increased almost linearly as a function of numbers of irradiating carbon ions, but it rarely depended on the cluster size. Cluster size effects were observed in the XRD peak intensity and the XRD peak width. With increasing the cluster size, the decrease in peak intensity becomes more remarkable and the peak width increases. The experimental result implies that the cluster ions with a larger size provide a more localized energy deposition in a sample, and cause larger and more inhomogeneous lattice disordering. As such, local and large lattice disordering acts as a pinning center for quantum vortex; energetic carbon-cluster ion irradiation will be effective for the increment in the critical current of $EuBa_2Cu_3O_{7-x}$ superconductors.

Keywords: $EuBa_2Cu_3O_{7-x}$ oxide superconductor; carbon-cluster ion irradiation; XRD spectra; lattice constant; lattice disordering

Citation: Iwase, A.; Saitoh, Y.; Chiba, A.; Hori, F.; Ishikawa, N. Effects of Energetic Carbon-Cluster Ion Irradiation on Lattice Structures of $EuBa_2Cu_3O_{7-x}$ Oxide Superconductor. *Quantum Beam Sci.* **2022**, *6*, 21. https://doi.org/10.3390/qubs6020021

Academic Editor: Elena Korznikova

Received: 12 April 2022
Accepted: 20 May 2022
Published: 25 May 2022

1. Introduction

As energetic cluster ion irradiation deposits very high-density energy into materials locally, when compared to the case of monoatomic ion irradiation, a lot of literature has reported the unique irradiation effects of cluster ions, such as large and non-linear emission yields of secondary ions and electrons from the surfaces [1–8], large sputtering yields [9–13], the production of gigantic craters and hillocks at target surfaces [6,14–21], and large ion-tracks inside the targets [6,18,22–31]. Energetic cluster ions also induce an exotic transformation of lattice structures from graphite to diamond [32], the large magnetization of a metallic alloy [33], and an anomalous mixing of metal precipitates and oxide matrix [34]. Although most of such cluster-irradiation effects have been analyzed in terms of high-density electronic excitation [3,15,17,19,20,22,24–27,30,32,34], several effects of cluster ion irradiation have been explained as a result of elastic collisions [8,10,13] or the synergy effect of electronic excitation and elastic collisions [12,23,29]. Concerning the modification of material structures by energetic cluster ions, they have mainly been observed as fine lattice structures by using a transmission microscope (TEM) and/or atomic force microscope (AFM). In this paper, we report the macroscopic change in lattice structures of the oxide superconductor, $EuBa_2Cu_3O_{7-x}$, irradiated with 0.5 MeV/atom C_1 monoatomic, C_4 cluster and C_8 cluster ions. The possibility of cluster ion irradiation as a tool for the improvement of the critical current is discussed. To the best of our knowledge, there are two papers that show the MeV cluster ion irradiation effect on oxide superconductors [31,35].

2. Experimental Procedure

Thin films of $EuBa_2Cu_3O_{7-x}$ 100 nm thick were produced on MgO substrates by using an RF-magnetron sputtering method [36]. The films were c-axis oriented and the superconducting transition temperature, T_c, was around 90 K [36]. The films were irradiated with 0.5 MeV C monoatomic ions, 2 MeV C_4 cluster ions and 4 MeV C_8 cluster ions using a tandem accelerator at Takasaki Advanced Accelerator Research Institute of National Institutes for Quantum Science and Technology (QST-Takasaki) [37]. The ion energy per carbon atom was the same for the monoatomic carbon ion and the two kinds of carbon-cluster ions (0.5 MeV/carbon atom). The samples were irradiated at room temperature, and along the normal of the film plane.

To observe the irradiation-induced change in lattice structures precisely, the X-ray diffraction (XRD) spectra were measured for each sample before and after the irradiation. The averaged values of the c-axis lattice constant were estimated by measuring the positions of (001) to (0010) XRD peaks and using the extrapolation function of Nelson and Riley [38].

Thus far, we examined the effect of monoatomic ion irradiation with the energy range of 0.85 MeV–3.8 GeV on the lattice constants of $EuBa_2Cu_3O_{7-x}$ [39–42]. The thickness of the samples used in our previous study was 300 nm. It is well known that cluster ions fragmentate into mono-atoms during the penetration in targets. To detect more precisely the effect of cluster ion irradiation, the cluster fragmentations have to be reduced as much as possible. Thus, the thickness of $EuBa_2Cu_3O_{7-x}$ samples for the present experiment was 100 nm, which was much smaller than that of our previous samples.

3. Results

Figure 1 shows the wide-scanned XRD spectrum for an unirradiated sample. We can observe several peaks corresponding to the crystal planes perpendicular to the c-axis (parallel to MgO substrate). High peaks around 43 and 95 degrees correspond to the MgO substrate.

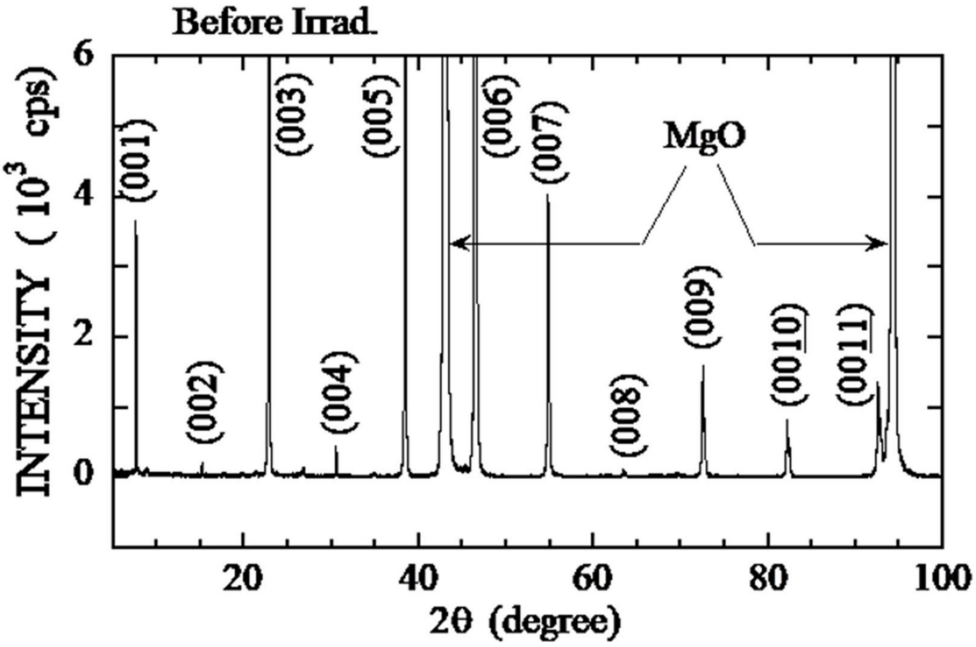

Figure 1. Wide-scanned XRD spectrum for the $EuBa_2Cu_3O_{7-x}$ film before irradiation.

Figure 2 shows the effects of C_1, C_4 and C_8 ion irradiation on (005) XRD peaks. The peaks shift to a lower angle with an increase in ion fluence. Other XRD diffraction peaks also shift to a lower-angle side by the irradiation. The present result indicates that the c-axis lattice constant increases by the irradiation. In Figure 3, the values of $\Delta c/c_0$ are plotted as a

function of ion fluence, Φ, where c_0 is the c-axis lattice constant before the irradiation, and $\Delta c = c(\Phi) - c_0$, the irradiation induced change in lattice constant. Here, we especially note the meaning of the ion fluence, Φ. It is the number of carbon atoms per cm^2, and not the number of cluster ions. To avoid any confusion, we call Φ as "carbon fluence" hereafter.

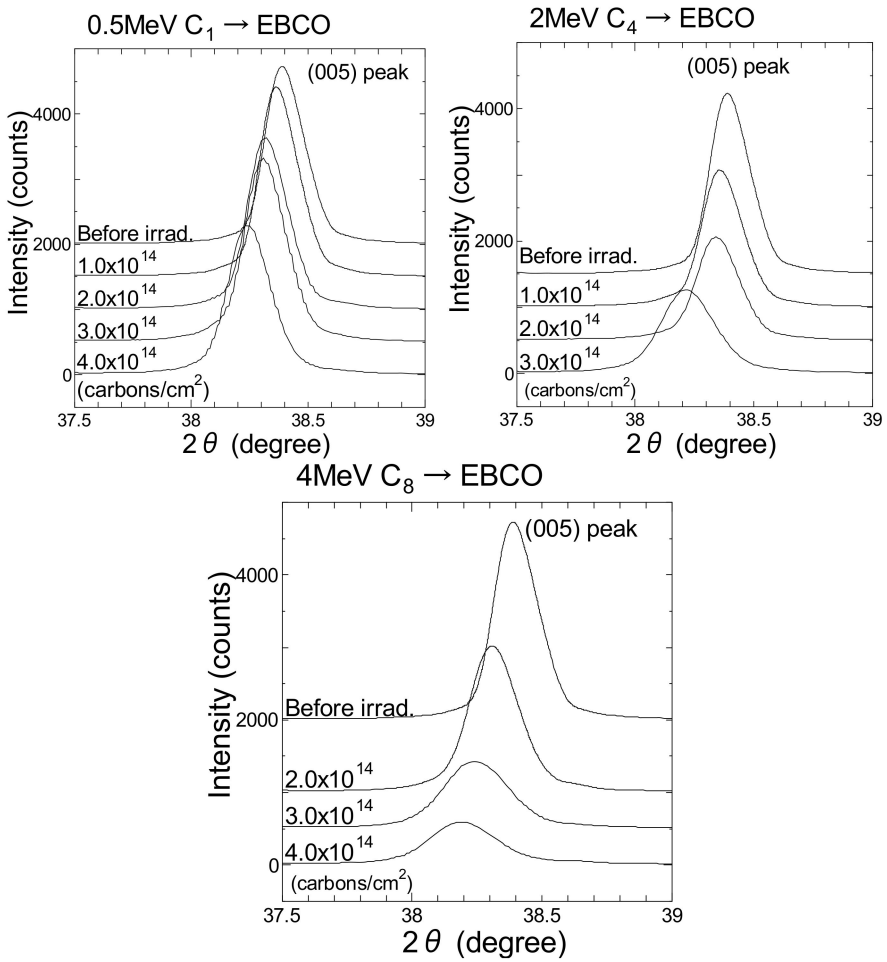

Figure 2. Change in (005) diffraction peaks for $EuBa_2Cu_3O_{7-x}$ films by 0.5 MeV C_1 monoatomic ion irradiation, 2 MeV C_4 and 4 MeV C_8 cluster ion irradiations. Carbon fluences are indicated in figures.

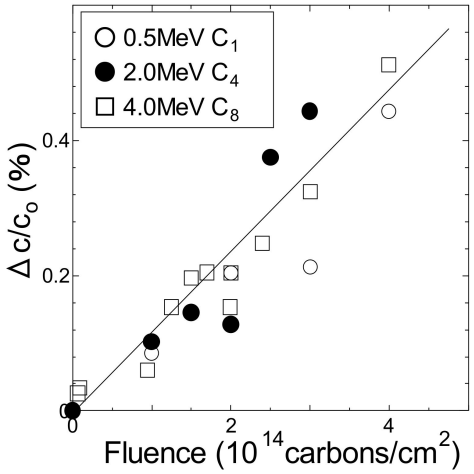

Figure 3. Irradiation-induced change in c-axis lattice constant normalized by the lattice constant before irradiation, c_0. Error bars for all the data points are smaller than the size of data symbols.

Although several data in Figure 3 are scattered to some extent, the values of $\Delta c/c_0$ increase almost linearly as a function of carbon fluence, and we do not find any systematic dependence of the c-axis lattice constant change on the cluster size.

In Figure 2, two other effects of the irradiation on the XRD spectra are observed. One is the decrease in peak intensity with increasing the ion fluence, and the other is the broadening of the peaks by the irradiation. Figure 4 indicates the intensity of (005) and (006) peaks, which is normalized by the peak intensity before the irradiation, as a function of carbon fluence.

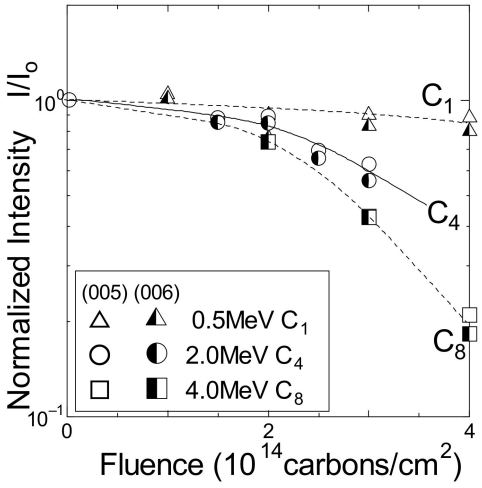

Figure 4. Normalized intensity for (005) and (006) peaks as a function of carbon fluence. Error bars for all the data points are smaller than the size of data symbols. Solid and dashed lines in the figure are a guide to the eye.

Unlike in the case of averaged c-axis lattice constant, the change in peak intensity by the irradiation shows a strong dependence on cluster size. The peak intensity decreases more rapidly for the irradiation with larger-sized carbon clusters.

The cluster-size dependence can also be found in the irradiation-induced broadening of the diffraction peaks. Figure 5 shows the values of full width at half maximum (FWHM) of (005) and (006) peaks, which are normalized by the value of FWHM before the irradiation, as a function of carbon fluence.

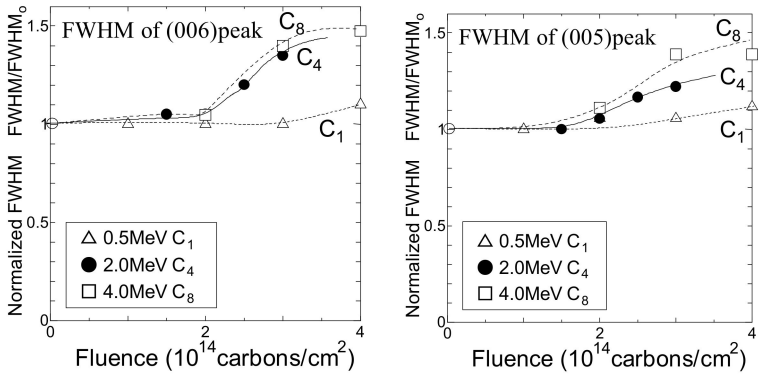

Figure 5. Normalized FWHM for (005) and (006) peaks as a function of carbon fluence. Error bars for all the data points are smaller than the size of data symbols. Solid and dashed lines in the figure are a guide to the eye.

As can be observed in the figure, the value of FWHM becomes larger for the irradiation with larger-sized carbon clusters.

4. Discussion

Thus far, we have reported the irradiation effect of several MeV monoatomic ions (0.85 MeV He, 1.0 MeV C, 0.95 MeV Ne and 2.0 MeV Ar) on the c-axis lattice constant of $EuBa_2Cu_3O_{7-x}$, and have shown that the increase in lattice constant, Δc, is proportional to the fluence of monoatomic ions, Φ [40]. In Figure 6, the normalized increments in the lattice constant for unit fluence, $(\Delta c/c_0)/\Phi$, are plotted against the nuclear stopping power, S_n. The values of S_n were obtained by using the SRIM calculation code [43]. In the figure, the present result for 0.5 MeV C_1 ions is also plotted.

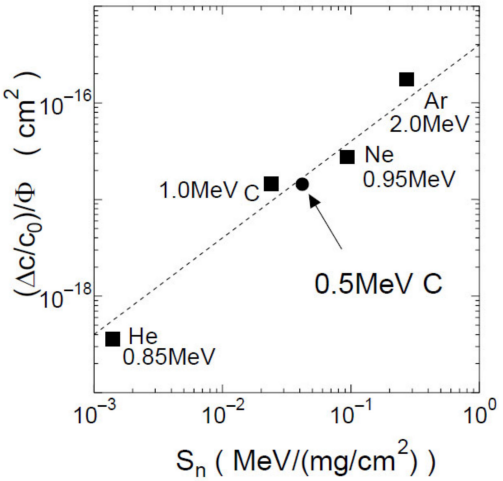

Figure 6. $(\Delta c/c_0)/\Phi$ as a function of S_n for the previous result of monoatomic He, C, Ne and Ar ion irradiation and the present result of 0.5 MeV C_1 ion irradiation. Data points for 2 MeV C_4 and 4 MeV C_8 cluster ions are placed on the data point for 0.5 MeV C_1 ions. Error bars for all the data points are smaller than the size of data symbols.

The figure shows that the irradiation-induced change in lattice constant for unit fluence is proportional to the value of S_n, regardless of ion species or energies:

$$(\Delta c/c_0)/\Phi = A \cdot S_n \tag{1}$$

where A is a constant. The value of S_n corresponds to the energy deposited into the sample by one irradiating ion through elastic collisions. For the irradiation with the fluence of Φ, the total energy deposited through the elastic collisions, E_D, is given as:

$$E_D = S_n \cdot \Phi \tag{2}$$

and the change in lattice constant, $\Delta c/c_0$, is:

$$\Delta c/c_0 = A \cdot S_n \cdot \Phi = A \cdot E_D \tag{3}$$

i.e., the change in lattice constant is proportional to the total energy deposited through the elastic collisions. As Figure 3 shows, the change in lattice constant for C_4 and C_8 cluster ion irradiation shows the same dependence on Φ as for C_1 monoatomic ion irradiation. Here, we confirm again that the meaning of Φ is the number of carbon atoms/cm^2 (carbon fluence). Therefore, data points for 2 MeV C_4 and 4 MeV C_8 cluster ions in Figure 6 are placed at the data point for 0.5 MeV C_1 ions, and the change in lattice constant, $\Delta c/c_0$, is determined only by the total energy deposited through the elastic collisions.

Although the irradiation-induced change in lattice constant does not show any cluster-size dependence, the changes in intensity and FWHM of the XRD peaks clearly depend on the cluster size. As can be observed in Figures 4 and 5, with increasing the cluster size, the peak intensity decreases, and the FWHM of the peaks increases. The C_4 and C_8 cluster ion

irradiation results in simultaneous collisions of 4–8 monoatomic carbon ions with target atoms, causing high-density energy deposition in narrow regions near the ion trajectories. With increasing the cluster size, the density of deposited energy becomes more localized and more inhomogeneous in space, although the total energy deposition is the same regardless of cluster size. The present result indicates that localized and inhomogeneous energy deposition by the cluster ions causes local lattice disordering, resulting in the decrease in XRD peak intensity and the peak broadening. On the other hand, the lattice constant decided by the XRD measurement corresponds to the averaged one over a wide area of the sample. Therefore, it is rarely affected by the local/inhomogeneous lattice disordering, but only depends on the total deposited energy by the irradiation.

$EuBa_2Cu_3O_{7-x}$ is one of $ReBa_2Cu_3O_{7-x}$ oxides, where Re is a rare-earth element, and a promising superconducting material for industrial applications because of the high superconducting transition temperature, T_c. The critical current density, J_c, under magnetic field (in-field J_c), which is a maximum current density with zero-resistivity, is the most important parameter for practical applications. It is well known that one-dimensional defective regions (ion-tracks) produced by swift heavy ion irradiation act as intense pinning centers for quantum vortices. A lot of studies for the modification of J_c have, therefore, been performed so far by irradiating $ReBa_2Cu_3O_{7-x}$ with GeV heavy ions ([44] and references therein). Recently, several papers have reported that much lower energy (about 100 keV-MeV) ion irradiation can also be used for the improvement of J_c of $ReBa_2Cu_3O_{7-x}$ superconductors [45–48]. The low-energy ion irradiation introduces point-like defects with a dimension of several nm. The lattice disordering inside and around the point-like defects act as effective pinning sites for quantum vortices. However, the energetic ion irradiation not only improves the critical currents, but also causes the degradation of superconductivity. The increase in the c-axis lattice constant of $ReBa_2Cu_3O_{7-x}$ by energetic ion irradiation is mainly caused by the deficiency of oxygen atoms [48]. The oxygen atom deficiency leads to the decrease in superconducting transition temperature, T_c. As the present experiment shows, under the condition of the same increase in c-axis lattice constant (the same oxygen deficiency), larger lattice disordering is locally induced by C-cluster ion irradiation as compared with monoatomic C-ion irradiation. Therefore, the present experimental result suggests that the MeV C-cluster ion irradiation will be useful for the improvement of J_c with less degradation of T_c.

5. Summary

$EuBa_2Cu_3O_{7-x}$ oxide films were irradiated with 0.5 MeV/atom C_1, C_4 and C_8 ions. The XRD spectra were measured before and after the irradiation. The c-axis increases almost proportionally with increasing carbon fluence, or energy deposited through elastic collisions and the cluster-size dependence is rarely observed. The irradiation also induces the decrease in XRD peak intensity and XRD peak broadening, which strongly depend on cluster size. With increasing the cluster size, the peak intensity decreases and the peaks become more broadened. The present experimental result shows that the change in averaged c-axis lattice constant is determined only by the total energy deposited through elastic collisions, but the larger cluster irradiation induces locally larger lattice disordering, which is due to localized and inhomogeneous energy deposition by the cluster ions.

Author Contributions: Conceptualization, N.I. and A.I.; formal analysis, N.I. and A.I.; ion irradiation experiment, Y.S. and A.C.; XRD measurements, N.I.; writing—original draft preparation, A.I.; writing—review and editing, N.I. and F.H. All authors have read and agreed to the published version of the manuscript.

Funding: A part of the study was supported by Inter-organizational Atomic Energy Research Program in an academic collaborative agreement among JAEA, QST, and the Univ. of Tokyo.

Data Availability Statement: Datasets acquired during the present research are available from the corresponding author on reasonable request.

Acknowledgments: The authors would like to thank O. Michikami for sample preparation. They also thank the technical staff at QST-Takasaki tandem accelerator facility for their help.

Conflicts of Interest: The authors declare no conflict of interest.

References

1. Benguerba, M.; Brunelle, A.; Della-Negra, S.; Depauw, J.; Joret, H.; Le Beyec, Y.; Blain, M.G.; Schweikert, E.A.; Ben Assayag, G.; Sudraud, P. Impact of slow gold clusters on various solids: Nonlinear effects in secondary ion emission. *Nucl. Instrum. Methods Phys. Res.* **1991**, *B62*, 8–22. [CrossRef]
2. Boussofiane-Baudin, K.; Brunelle, A.; Chaurand, P.; Della-Negra, S.; Depauw, J.; Hakansson, P.; Le Beyec, Y. Non-linear sputtering effects induced by MeV energy gold clusters. *Nucl. Instrum. Methods Phys. Res.* **1994**, *B88*, 61–68. [CrossRef]
3. Baudin, K.; Brunelle, A.; Della-Negra, S.; Depauw, J.; Le Beyec, Y.; Parilis, E.S. Sublinear effect in electron emission from solids bombarded with swift gold clusters. *Nucl. Instrum. Methods Phys. Res.* **1996**, *B117*, 47–54. [CrossRef]
4. Hirata, K.; Saitoh, Y.; Chiba, A.; Yamada, K.; Narumi, K. Time-of-Flight secondary ion mass spectrometry with energetic cluster ion impact ionization for highly sensitive chemical structure characterization. *Nucl. Instrum. Methods Phys. Res.* **2013**, *B314*, 39–42. [CrossRef]
5. Hirata, K.; Yamada, K.; Chiba, A.; Hirano, Y.; Saitoh, Y. Secondary ion mass spectrometry using energetic cluster ion beams: Toward highly sensitive imaging mass spectrometry. *Nucl. Instrum. Methods Phys. Res.* **2020**, *B479*, 240–245. [CrossRef]
6. Brunelle, A.; Della-Negra, S.; Depauw, J.; Jacquet, D.; Le Beyec, Y.; Pautrat, M.; Schoppmann, C. Collisions of fast clusters with solids and related phenomena. *Nucl. Instrum. Methods Phys. Res.* **1997**, *B125*, 207–213. [CrossRef]
7. Lai, T.L.; Jacquet, D.; Ribaud, I.; Eller, M.J.; Verkhoturov, D.; Schweikert, E.A.; Tizei, L.H.G.; Shao, F.; Bilgen, S.; Mercier, B.; et al. Enhanced sputter and secondary ion yields using MeV gold nanoparticle beams delivered by the Andromede facility. *J. Vac. Sci. Technol.* **2020**, *B38*, 044008. [CrossRef]
8. Bouneau, S.; Della-Negra, S.; Jacquet, D.; Le Beyec, Y.; Pautrat, M.; Shapiro, M.H.; Tombrello, T.A. Measurement of energy and angular distributions of secondary ions in the sputtering of gold by swift Au_n clusters: Study of emission mechanisms. *Phys. Rev.* **2005**, *B71*, 174110. [CrossRef]
9. Baudin, K.; Brunelle, A.; Della-Negra, S.; Jacquet, D.; Hakansson, P.; Le Beyec, Y.; Pautrat, M.; Pinho, R.R.; Schoppmann, C. Sputtering of large size clusters from solids bombarded by high energy cluster ions and fullerenes. *Nucl. Instrum. Methods Phys. Res.* **1996**, *B112*, 59–63. [CrossRef]
10. Beranov, I.; Della-Negra, S.; Domaratsky, V.; Chemezov, A.; Novikov, A.; Obnorsky, V.; Pautrat, M.; Anders, C.; Urbassek, H.M.; Wien, K.; et al. Desorption of nanoclusters from gold nanodispersed layers by 72 keV Au400 ions: Experimental and molecular dynamics simulation. *Nucl. Instrum. Methods Phys. Res.* **2008**, *B266*, 1993–2001. [CrossRef]
11. Andersen, H.H.; Brunelle, A.; Della-Negra, S.; Depauw, J.; Jacquet, D.; Le Beyec, Y.; Chaumont, J.; Bernas, H. Giant Metal Sputtering Yields Induced by 20–5000 keV/atom Gold Clusters. *Phys. Rev. Lett.* **1998**, *80*, 5433–5436. [CrossRef]
12. Amekura, H.; Narumi, K.; Chiba, A.; Hirano, Y.; Yamada, K.; Tsuya, D.; Yamamoto, S.; Okubo, N.; Ishikawa, N.; Saitoh, Y. C_{60} ions of 1 MeV are slow but elongate nanoparticles like swift heavy ions of hundreds MeV. *Sci. Rep.* **2019**, *9*, 14980. [CrossRef]
13. Narumi, K.; Naramoto, H.; Yamada, K.; Chiba, A.; Saitoh, Y. Sputtering Yields of Si Bombarded with 10–540-keV C_{60} Ions. *Quantum Beam Sci.* **2022**, *6*, 12. [CrossRef]
14. Barlo Daya, D.D.N.; Hallen, A.; Eriksson, J.; Kopniczky, J.; Papaleo, R.; Reimann, C.T.; Hakansson, P.; Sundqvist, B.U.R.; Brunelle, A.; Della-Negra, S.; et al. Radiation damage features on mica and L-valine probed by scanning force microscopy. *Nucl. Instrum. Methods Phys. Res.* **1995**, *B106*, 38–42. [CrossRef]
15. El-Said, A.S.; Aumayr, F.; Della-Negra, S.; Neumann, R.; Schwartz, K.; Toulemonde, M.; Trautmann, C.; Voss, K.-O. Scanning force microscopy of surface damage created by fast C_{60} cluster ions in CaF_2 and LaF_3 single crystals. *Nucl. Instrum. Methods Phys. Res.* **2007**, *B256*, 313–318. [CrossRef]
16. Girard, J.C.; Michel, A.; Tromas, C.; Jaouen, C.; Della-Negra, S. Track formation in amorphous $Fe_{0.55}Zr_{0.45}$ alloys irradiated by MeV C_{60} ions: Influence of intrinsic stress on induced surface deformations. *Nucl. Instrum. Methods Phys. Res.* **2003**, *B209*, 85–92. [CrossRef]
17. El-Said, A.S. Tracks of 30-MeV C_{60} clusters in yttrium iron garnet studied by scanning force microscopy. *Nucl. Instrum. Methods Phys. Res.* **2009**, *B267*, 953–956. [CrossRef]
18. Jensen, J.; Dunlop, A.; Della-Negra, S.; Pascard, H. Tracks in YIG induced by MeV C_{60} ions. *Nucl. Instrum. Methods Phys. Res.* **1998**, *B135*, 295–301. [CrossRef]
19. Barlo Daya, D.D.N.; Reimann, C.T.; Hakansson, P.; Sundqvist, B.U.R.; Brunelle, A.; Della-Negra, S.; Le Beyec, Y. Crater formation due to grazing incidence C_{60} cluster ion impacts on mica: A trapping-mode scanning force microscopy study. *Nucl. Instrum. Methods Phys. Res.* **1997**, *B124*, 484–489. [CrossRef]
20. Döbeli, M.; Ames, F.; Musil, C.R.; Scandella, L.; Suter, M.; Synal, H.A. Surface tracks by MeV C_{60} impacts on mica and PMMA. *Nucl. Instrum. Methods Phys. Res.* **1998**, *B143*, 503–512. [CrossRef]
21. Henry, J.; Dunlop, A.; Della-Negra, S. Craters, bumps and onion structures in MoS_2 irradiated with MeV C_{60} ions. *Nucl. Instrum. Methods Phys. Res.* **1998**, *B146*, 405–411. [CrossRef]

22. Jensen, J.; Dunlop, A.; Della-Negra, S.; Toulemonde, M. A comparison between tracks created by high energy mono-atomic and cluster ions in $Y_3Fe_5O_{12}$. *Nucl. Instrum. Methods Phys. Res.* **1998**, *B146*, 412–419. [CrossRef]
23. Kitayama, T.; Morita, Y.; Nakajima, K.; Narumi, K.; Saitoh, Y.; Matsuda, M.; Sataka, M.; Tsujimoto, M.; Isoda, S.; Toulemonde, M.; et al. Formation of ion tracks in amorphous silicon nitride films with MeV C_{60} ions. *Nucl. Instrum. Methods Phys. Res.* **2015**, *B356–357*, 22–27. [CrossRef]
24. Jensen, J.; Dunlop, A.; Della-Negra, S. Tracks induced in CaF_2 by MeV cluster irradiation. *Nucl. Instrum. Methods Phys. Res.* **1998**, *B141*, 753–762. [CrossRef]
25. Dunlop, A.; Jaskierowicz, G.; Della-Negra, S. Latent track formation in silicon irradiated by 30 MeV fullerenes. *Nucl. Instrum. Methods Phys. Res.* **1998**, *B146*, 302–308. [CrossRef]
26. Canut, B.; Bonardi, N.; Ramos, S.M.M.; Della-Negra, S. Latent tracks formation in silicon single crystals irradiated with fullerenes in the electronic regime. *Nucl. Instrum. Methods Phys. Res.* **1998**, *B146*, 296–301. [CrossRef]
27. Sall, M.; Monnet, I.; Moisy, F.; Grygiel, C.; Jublot-Leclerc, S.; Della-Negra, S.; Toulemonde, M.; Balanzat, E. Track formation in III-N semiconductors irradiated by swift heavy ions and fullerene and re-evaluation of the inelastic thermal spike model. *J. Mater. Sci.* **2015**, *50*, 5214–5227. [CrossRef]
28. Dammak, H.; Dunlop, A.; Lesueur, D.; Brunelle, A.; Della-Negra, S.; Le Beyec, Y. Tracks in Metals by MeV Fullerenes. *Phy. Rev. Lett.* **1995**, *74*, 1135–1138. [CrossRef]
29. Amekura, H.; Toulemonde, M.; Narumi, K.; Li, R.; Chiba, A.; Hirano, Y.; Yamada, K.; Yamamoto, S.; Ishikawa, N.; Okubo, N.; et al. Ion tracks in silicon formed by much lower energy deposition than the track formation threshold. *Sci. Rep.* **2021**, *11*, 185. [CrossRef]
30. Dhamodaran, S.; Pathak, A.P.; Dunlop, A.; Jaskierowicz, G.; Della-Negra, S. Energetic cluster irradiation of InP. *Nucl. Instrum. Methods Phys. Res.* **2007**, *B256*, 229–232. [CrossRef]
31. Ishikawa, N.; Van der Beek, C.J.; Dunlop, A.; Jaskierowicz, G.; Li, M.; Kes, P.H.; Della-Negra, S. Vortex Phase Diagram in $Bi_2Sr_2CaCu_2O_{8+\delta}$ with Damage Tracks Created by 30 MeV Fullerene Irradiation. *J. Phys. Soc. Jpn.* **2004**, *73*, 2813–2821. [CrossRef]
32. Dunlop, A.; Jaskierowicz, G.; Ossi, P.M.; Della-Negra, S. Transformation of graphite into nanodiamond following extreme electronic excitation. *Phys. Rev.* **2007**, *B76*, 155403. [CrossRef]
33. Koide, T.; Saitoh, Y.; Sakamaki, M.; Amemiya, K.; Iwase, A.; Matsui, T. Change in magnetic and structural properties of FeRh thin films by gold cluster ion beam irradiation with the energy of 1.67 MeV/atom. *J. Appl. Phys.* **2014**, *115*, 17B722. [CrossRef]
34. Beranger, M.; Thevenard, P.; Brenier, R.; Canut, B.; Ramos, S.M.M.; Brunelle, A.; Della-Negra, S.; Le Beyec, Y.; Balanzat, E.; Tombrello, T. Ion-beam mixing induced by atomic and cluster bombardment in the electronic stopping-power regime. *Phys. Rev.* **1996**, *B53*, 14773–14781. [CrossRef]
35. Tomaschko, C.; Schoppmann, C.; Kraus, M.; Kragler, K.; Kreiselmeyer, G.; Saemann-Ischenko, G.; Voit, H.; Brunelle, A.; Della-Negra, S.; Le Beyec, Y. MeV cluster ion induced defect production in high Tc superconductors. *Nucl. Instrum. Methods Phys. Res.* **1996**, *B117*, 90–94. [CrossRef]
36. Michikami, O.; Asahi, M.; Asano, H. Superconducting and Structural Properties of $EuBa_2Cu_3O_{7-\delta}$ Ultrathin Films Deposited on MgO(100) Substrates Using Magnetron Sputtering. *Jpn. J. Appl. Phys.* **1990**, *29*, L298–L301. [CrossRef]
37. Saitoh, Y.; Mizuhashi, K.; Tajima, S. Acceleration of cluster and molecular ions by TIARA 3 MV tandem accelerator. *Nucl. Instrum. Methods Phys. Res.* **2000**, *A452*, 61–66. [CrossRef]
38. Nelson, J.B.; Riley, D.P. An experimental investigation of extrapolation methods in the derivation of accurate unit-cell dimensions of crystals. *Proc. Phys. Soc.* **1945**, *57*, 160–177. [CrossRef]
39. Ishikawa, N.; Iwase, A.; Chimi, Y.; Maeta, H.; Tsuru, K.; Michikami, O. Lattice expansion in $EuBa_2Cu_3O_y$ irradiated with energetic ions. *Physica* **1996**, *C259*, 54–56. [CrossRef]
40. Ishikawa, N.; Chimi, Y.; Iwase, A.; Maeta, H.; Tsuru, K.; Michikami, O.; Kambara, T.; Mitamura, T.; Awaya, Y.; Terasawa, M. Electronic excitation effects in ion-irradiated high-T_c superconductors. *Nucl. Instrum. Methods Phys. Res.* **1998**, *B135*, 184–189. [CrossRef]
41. Iwase, A.; Ishikawa, N.; Chimi, Y.; Tsuru, K.; Wakana, H.; Michikami, O.; Kambara, T. High energy heavy ion irradiation damage in oxide superconductor $EuBa_2Cu_3O_y$. *Nucl. Instrum. Methods Phys. Res.* **1998**, *B146*, 557–564. [CrossRef]
42. Ishikawa, N.; Iwase, A.; Chimi, Y.; Michikami, O.; Wakana, H.; Hashimoto, T.; Kambara, T.; Muller, C.; Neumann, R. Se-scaling of lattice parameter change in high ion-velocity region ($v > 2.6 \times 10^9$ cm/s) in ion-irradiated $EuBa_2Cu_3O_y$. *Nucl. Instrum. Methods Phys. Res.* **2002**, *B193*, 278–282. [CrossRef]
43. Ziegler, J. Available online: https://www.srim.org/ (accessed on 20 March 2022).
44. Sueyoshi, T. Modification of Critical Current Density Anisotropy in High-T_c Superconductors by Using Heavy-Ion Irradiations. *Quantum Beam Sci.* **2021**, *5*, 16. [CrossRef]
45. Matsui, H.; Ogiso, H.; Yamasaki, H.; Kumagai, T.; Sohma, M.; Yamaguchi, I.; Manabe, T. 4-fold enhancement in the critical current density of $YBa_2Cu_3O_7$ films by practical ion irradiation. *Appl. Phys. Lett.* **2012**, *101*, 232601. [CrossRef]
46. Jia, Y.; LeRoux, M.; Miller, D.J.; Wen, J.G.; Kwok, W.K.; Welp, U.; Rupich, M.W.; Li, X.; Sathyamurthy, S.; Fleshler, S.; et al. Doubling the critical current density of high temperature superconducting coated conductors through proton irradiation. *Appl. Phys. Lett.* **2013**, *103*, 122601. [CrossRef]

47. Leroux, M.; Kihlstrom, K.J.; Holleis, S.; Rupich, M.W.; Sathyamurthy, S.; Fleshler, S.; Sheng, H.P.; Miller, D.J.; Eley, S.; Civale, L.; et al. Rapid doubling of the critical current of $YBa_2Cu_3O_{7-\delta}$ coated conductors for a viable high-speed industrial processing. *Appl. Phys. Lett.* **2015**, *107*, 192601. [CrossRef]
48. Huang, D.; Gu, H.; Shang, H.; Li, T.; Xie, B.; Zou, Q.; Chen, D.; Chu, W.K.; Ding, F. Enhancement in the critical current density of $BaTiO_3$-doped YBCO films by low-energy (60 keV) proton irradiation. *Supercond. Sci. Technol.* **2021**, *34*, 045001. [CrossRef]